Chapter

Study of Equatorial Plasma Bubbles Using ASI and GPS Systems

Dada P. Nade, Swapnil S. Potdar and Rani P. Pawar

Abstract

The plasma irregularities have been frequently observed in the F-region, at low latitude regions, due to the instability processes occurring in the ionosphere. The depletions in electron density, as compared to the background density, is a signature of the plasma irregularities. These irregularities are also known as the "equatorial plasma bubble" (EPB). These EPBs can measure by the total electron content (TEC) using GPS receiver and by images of the nightglow OI 630.0 nm emissions using all sky imager (ASI). The current chapter is based on the review on the signature of the EPBs in TEC and ASI. measurements. We have also discussed the importance of the study of EPBs.

Keywords: EPB, plasma irregularities, GPS and TEC

1. Introduction

The ionospheric radio wave communication, especially navigation is strongly influenced by the equatorial spread-F irregularities. Therefore, it is a scientific interest to do study these irregularities and its morphology and dynamic for the better communication system. The equatorial spread-F irregularities have been studied by several investigators using number of measurement techniques (e.g., [1–3]). The ground-based measurement techniques such as all sky imager (ASI), scanning photometer, RADAR and ionosonde are mostly used to study the dynamics of these irregularities. In equatorial-low latitude F-region, the electron density is depletes or enhance with respect to the background density due to vertical dynamics of F region. This is a key factor for generation of ionospheric irregularities. The size of these domains of irregularities ranges from a few hundred of kilometers in the east-west direction [4, 5] and a thousands of kilometers in north-south direction aligned with magnetic field lines (e.g., [6]). Basically, they occurred in the low latitude F region over an altitude 250–350 km, such irregularities have observed as dark and bright patches in the nightglow images of OI 630.0 nm emission. The dark patches are also called as equatorial plasma bubbles (EPBs) (e.g., [7, 8]) and bright patches are called as plasma blobs (e.g., [9, 10]).

Few investigators have been reported the nocturnal variations in occurrence (e.g., [7, 11, 12]) and zonal drift velocity (e.g., [8, 13]) of EPBs using OI 630.0 nm images. Many researchers have addressed generation mechanism of EPBs using different techniques (e.g., [14–16]). According to them, the EPBs are generated in the

bottom side of F-region (e.g., [9, 17]) at the equator, mainly by the nonlinear evolution of the generalized Rayleigh-Taylor (GRT) instability [18] and E × B drift [14]. After sunset, the rapid uplifting of F-region is one of the key factors in generating of EPBs [19, 20].

The first time observation of plasma blobs has made with images of OI 630.0 nm, which were taken by the ground-based ASI from Cachoeira Paulista [21]. Using the similar data from the Boston University, Arecibo, Krall et al. [22] have also reported the observations of plasma blobs. The general characteristics of plasma blobs have been studied by using measurements of total electron content (TEC) [23].

Nade et al. [10], suggested that the plasma blobs occurred with EPBs and the variations in apex height may responsible for occurrence of the plasma blobs over low latitude region. However, the generation mechanism of EPBs and plasma blobs is not yet clearly understood [24] and it is most challenging issue to study the dynamics of the low latitude F region. In addition, several questions were raised by Kil et al. [25] on the EPB-blob connection. They reported that the creation of plasma blobs is not depending on EPBs and they also mentioned that the occurrence rate of EPBs varies with solar activity while blobs occurred frequently with solar activity. Based on these results they raised the question, why the occurrence of plasma blobs shows opposite nature with solar activity? These questions are creating inspiration to do more research in the same area.

2. Methodology

2.1 Nightglow emission OI 630.0 nm measurement

Based on numerous ground-based and in-situ studies, it is widely accepted that the nightglow OI 630.0 nm emissions are generated at low latitude F-region heights (250–300 km). The nightglow emission in F-region at (1D) 630.0 nm is governed by dissociative recombination between ions and electrons [26, 27]. The nightglow OI 630.0 nm images are used to study the characteristics of EPBs. Otsuka et al. [28] suggested that the ASI is an important aide towards improving the understanding of the coupling between ionosphere and thermosphere using images of nightglow OI 630.0 nm emission and OH emission. Because OH emissions are generating at around 100 km (ionosphere) while OI 630.0 nm emissions are generating at around 250 km (thermosphere).

Few methods are available in literature to analyze the all sky image data [29, 30]. Kubota et al. [31] has introduced a new method to convert the pixel images of the ASI into actual geographic coordinates for 250 km altitude, the airglow emission layer. Then to retrieve information from image data, the pixel value of images converted into corresponding latitude-longitude values by Narayanan et al. [32]. Recently, by the combination of both methods, Sharma et al. [33] has introduced the "average method" to process and analyze the image data.

Figure 1 illustrates processed images of OI 630.0 nm, which are taken on 17-18 January, 2012, showing the time evolution and structure of the EPBs and plasma blobs. In **Figure 1**, yellow and white arrows are showing signature of EPB and plasma blobs respectively in the OI 630.0 nm images.

To retrieve the pixel intensity from images of nightglow OI 630.0 nm Taori et al. [34] has introduced "the image crop method." In this method, we have selected only a square bin of 5 × 5 pixel at the center of the image corresponding to a rectangular field of view having ~1° along the zenith. The average intensity of this square bin is considered as intensity of OI 630.0 nm emission to study the nocturnal variation in

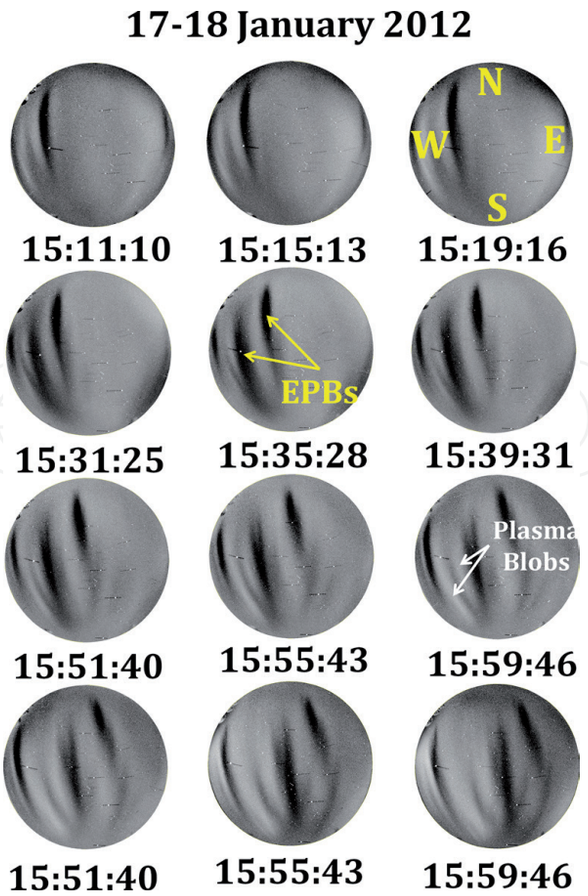

Figure 1.
Sequences of images of OI 630.0 nm obtained on 17-18 January, 2012 in IST at Kolhapur. Yellow and white arrows are showing dark and bright (EPB and plasma blob) respective structures in images.

intensity. Thus, we got the intensity data of OI 630.0 nm emission for each individual image with respect to time.

2.2 TEC measurements

Up to 11 GPS satellites are in view and provide outputs in 22 receiver channels [35]. The ionosphere has an effect on the signal of GPS satellite. TEC is measured along the path from the GPS satellite to a receiver. The TEC is defined by the integral of electron density in TEC unit (TECU), where $1\ TEC\ unit = 10^{16} electrons/m^2$ column along the signal transmission path. The dual frequency GPS receivers are used to measure the TEC, which is one of the most important methods to investigate the dynamics of ionosphere. Several research groups are showing interest in the equatorial ionospheric research using GPS data. Dow et al. [36] did an analysis of the importance of GPS data in support of the terrestrial reference frame, earth observations and research, positioning, navigation and timing as well as other applications that benefit the society. The slant TEC is the measure of the total number of free electrons in a column of unit cross section along the path of the electromagnetic wave between the satellite and the receiver [37].

A dual frequency (L1 = 1575.42 MHz and L2 = 1227.60 MHz) GPS receiver (LEICA GRX1200GGPRO GNSS) is operating at Hyderabad (17.37°N, 78.48°E) [3]. It is a unique station to study the ionospheric irregularities because it is located at the northern crest of the equatorial ionization anomaly (EIA). A dual-frequency GPS receiver can measure the difference in ionospheric delays between the L1 and L2 of the GPS frequencies, which are generally assumed to travel along the same path through the ionosphere. Thus, the group delay can be obtained as

$$\Delta(\delta t) = \delta t_{L1} - \delta t_{L2} \tag{1}$$

Here, $\Delta(\delta t)$ is a time delay in the pseudo-range (δt_{L1}) at L1 and pseudo-range (δt_{L1}) at L2. The resulting equation is (Jain et al., 2011),

$$\Delta(\delta t) = 40.3 \times TEC \times \frac{\left(f_{L1}^2 - f_{L2}^2\right)}{c \times f_{L1}^2 \times f_{L2}^2} \tag{2}$$

where f_{L1} and f_{L2} are the group path lengths corresponding to the high and low GPS frequencies $f_{L1} = 1575.42\ MHz$ and $f_{L2} = 1227.60\ MHz$, respectively and "c" is speed of light in vacuum. The TEC can be obtained by rewrite above equation as,

$$TEC = \frac{1}{40.3} \times \frac{c \times f_{L1}^2 \times f_{L2}^2}{\left(f_{L1}^2 - f_{L2}^2\right)} \times \Delta(\delta t) \tag{3}$$

The signal from different GPS satellites, at random elevation angles, recorded as a TEC measurements. These different satellites are identified by a pseudo-random number (PRN). The portions of the ionosphere cross by GPS signal depend on the elevation angle of GPS satellite. Therefore, in the present work the TEC data of only those GPS satellites, having elevation angles above 30° to avoid the multipath effect of signals, are considered. The maximum elevation angle over Hyderabad station is 60°. The STEC is measured at every 30 s by the GPS receiver.

3. Equatorial plasma bubble by GPS

The study of the spatial and temporal progress of EPBs formed in the ionosphere has been carried out using two different techniques radio waves as well as optical imaging over the globe. The optical imaging techniques have a limited coverage area, but have high resolution, while the radio wave techniques have a wide coverage area but can have low resolution for the ionospheric studies. The all sky imager is widely used instrument for the optical imaging of plasma bubble while GPS receivers used to study the ionospheric irregularities using radio waves. The **Figure 2** illustrates the occurrence of EPBs as D1 and D2 in the TEC measurements. The nocturnal variation in TEC with respect to local time (Indian Standard Time) observed on April 1, 2011 and April 2, 2011. The EPBs in TEC is indicated by D1 and D2. The occurrence period of EPBs is indicated by rectangular in the **Figure 2**.

Nishioka et al. [38] did a comprehensive study of the occurrence of plasma bubbles using ground-based GPS receiver from dip equator stations. They have considered Data from 2000 to 2006 from a network of 23 GPS receivers such as network of International GNSS Service (IGS), a GPS network by the Japan Agency for Marine-Earth Science and Technology (JAMSTEC), and Scripps Orbit Permanent Array Center (SOPAC), etc. They found a different characteristic rate of EPB occurrence in different regions also the dependency of the occurrence on the solar activity was different among the regions. They concluded that the sunset time lag effect plays an important role for the monthly variation and two asymmetries which could not be explained with the sunset time lag scenario (1) asymmetry between two solstices and (2) asymmetry between two equinoxes. They also found that the plasma bubble occurrence was high and constant for a stations having height on the dip equator (HODE) was <700 km and it is began to decrease for stations having HODE was higher than 700 km and was almost zero for the stations having HODE

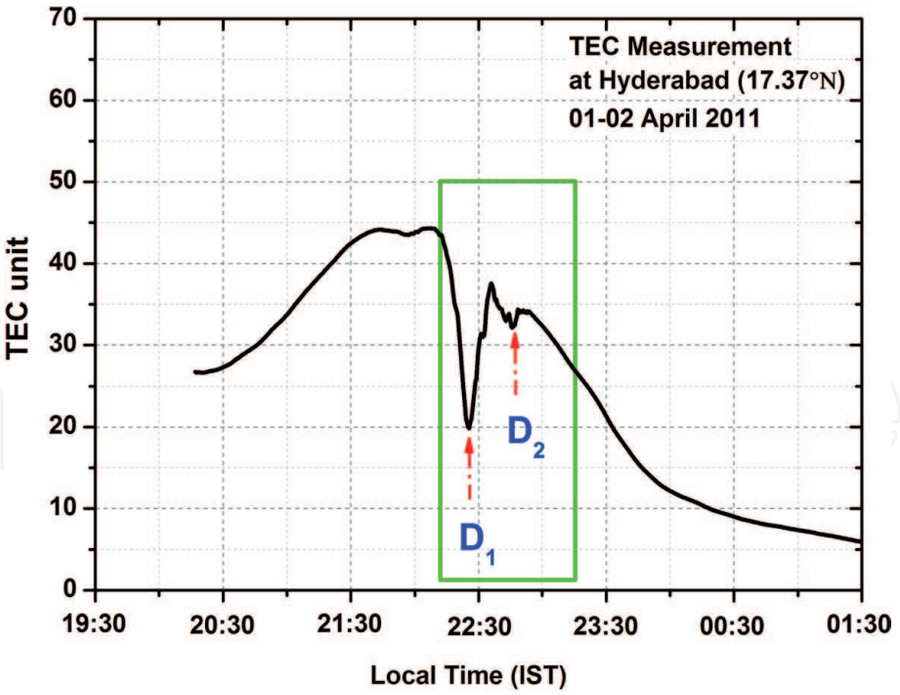

Figure 2.
The nocturnal variation in TEC with respect to local time (Indian Standard Time) observed on 01-02 April 2011. The EPBs in TEC is indicated by D_1 and D_2. The occurrence period of EPBs is indicated by rectangular.

higher than 900 km.. They defined HODE as shown in figure as an altitude of the geomagnetic field line on the magnetic dip equator which passes 400 km altitude above a site of GPS receiver.

Haase et al. [39] have studied the Propagation of plasma bubbles over Brazil from GPS and airglow data. They have mapped the airglow data to the GPS line-of-sight geometry for the direct comparison and revealing of resolvable westward tilt of the plasma depletion that may be due to vertical shear. They found the direct correspondence between integrated electron content (IEC) depletions and characteristics of depletions seen in horizontal airglow images, with very consistent observations of scale, amplitude, drift velocity and timing.

The EPB is monitored by using data provided by ground-based GNSS receiver Network over the South American continent by Takahashi et al. [40]. They have mapped the total electron content which could cover almost all of the continent within 4000 km distance in longitude and latitude. The TEC variability is monitored continuously with a time resolution of 10 min. The bubble structures are compared with simultaneous observations of OI630 nm all-sky image at Cachoeira Paulista (22.7°S, 45.0°W) and Cariri (7.4°S, 36.5°W). The formation and development of the bubble and eastward drifting features were successfully monitored and analyzed in this study. They found that the plasma bubbles observed during the December solstice has a periodic spacing, which is a periodic seeding mechanism of the bubbles.

The occurrence and characteristics of EPBs have been analyzed using the TEC data from GPS receivers over Hong Kong during 2001–2012 by Kumar et al. [41]. They found that the maximum occurrences of EPBs during the equinoctial months while minimum during the December solstice throughout 2001–2012. They also used the TEC data from different GNSS receivers over the Hong Kong. They concluded that the asymmetry in the EPB occurrences could be caused by the suppression of the growth rate of the instability by inter hemispheric neutral winds, which is known to be a primary cause for triggering EPB or ESF. The influence of solar and magnetic cycle is also studied.

Magdaleno et al. [42] studied the Climatology characterization of EPB using GPS data for the period 1998–2008. They have considered the slant total electron content (sTEC) derived from global positioning system (GPS) data from 67 International GNSS Service (IGS) stations distributed worldwide around the geomagnetic equator and the region of the ionospheric equatorial anomaly (IEA). The Ionospheric Bubble Seeker method is used to detect and distinguishes TEC depletions associated with EPBs. They found the largest occurrence rate of EPBs over the South America-Africa region and shown that the occurrence rate goes on decreasing as we go from the magnetic equator to higher latitudes.

First time study of the occurrence frequency of EPB over West Africa is done by Okoh et al. [42] using an ASI and GNSS Receivers from June 9, 2015 to January 31, 2017. This ASI is installed at Abuja (Geographic: 8.99°N, 7.38°E; Geomagnetic: 1.60°S) which covers almost the entire airspace of Nigeria. They found most occurrences of EPB during equinoxes and least occurrences during solstices also the occurrence rate of EPBs were highest around local midnight and lower for hours farther away. They also observed that the on/off status of EPB in airglow and GNSS observations are in 70% agreement.

Kumar [43] has studied the morphology of the EPB with respect of the solar activity over the Indian region from 2007 to 2012. The sTEC data are also considered from ground-based GPS receiver at Hyderabad (17.41° N, 78.55° E, Mag Lat 08.81° N) and two receivers at Bangalore (13.02°/13.03° N, 77.57°/77.51° E, Mag. Lat. 04.53°/04.55° N) in Indian region. He also observes that the occurrence of EPB is maximum in equinoctial months. He concluded that the equinox maximum in EPB occurrences for high solar activity years may be caused by the vertical F-layer drift due to pre-reversal electric field (PRE). This is expected to be maximum when daynight terminator aligns with the magnetic meridian, i.e., during the equinox months, whereas maximum occurrences during the solstice months of solar minimum could be caused by the seed perturbation in plasma density induced by gravity waves from tropospheric origins. The seasonal dependence of the EPBs occurrence is also studied.

Recently, Takahashi et al. [44] in detail studied the Occurrences of EPB (EPBs) and medium-scale traveling ionospheric disturbances (MSTIDs). They have used the GPS satellite data-based total electron content mapping, ionograms, and 630 nm all-sky airglow images observed over the South American continent during the period of 2014–2015. They observed a close relationship between the inter-bubble distance and the horizontal wavelength of the MSTIDs. They concluded that the MSTIDs are followed by EPBs primarily in the afternoon to the evening period due to the strong tropospheric convective activities (cold fronts and/or intertropical convergence zones) and the MSTIDs could be one of the seeding sources of EPBs.

Barros et al. [45] used ground-based network of GNSS receivers used to monitor EPB (EPBs) by mapping the total electron content (TEC map). They considered TEC data from GNSS receivers over South America for the period between November 2012 and January 2016. They found the latitudinal gradient varying from 123 ms^{-1} at the Equator to 65 ms^{-1} for 35° S latitude in the zonal drift velocities of the EPBs. They concluded that the latitudinal gradient in the inter-bubble distances seems to be related to the difference in the zonal drift velocity of the EPB from the Equator to middle latitudes and to the difference in the westward movement of the terminator.

Over the Thailand region, the statistical analysis of the separation distance between EPB is carried by Bumrungkit et al. [46]. The separation distance between EPBs is calculated using the Haversine formula technique in which the dual frequency GPS signal used. Their results show that the separation distances between EPBs on disturbed days in 2015 are in the range of 100–1200 km.

The effects of the R-T instability and EPB on the GPS signal are also studied by Panda et al. [47]. They have considered various instances of ionospheric disturbances triggered by natural processes such as earthquakes and volcanic eruption in the recent decade to investigate the spatiotemporal and seasonal effects of ionospheric irregularities on the GNSS signals. They found that the co-seismic ionospheric disturbances are difficult to study at the equatorial region due to mask of the EPBs but over the high latitude region these co-seismic ionospheric anomaly van be studied.

The effects of plasma bubbles on the GPS signal path and the positioning issue is studied by Moraes et al. [48]. The analysis focused on data from November 15, 2014 to November 30, 2014 and from February 4, 2015 to February 18, 2015, at São José DOS Campos, Brazil. They found that passing through the EPB, the radio signal may take a longer propagation path and have more losses of signal lock. The positioning errors may result in these cases.

Rajesh et al. [49] demonstrate that the EPBs appear to extend toward equator or pole as a result of the descending F layer and the recombination between free electrons of F layer and ions of the E layer at different latitudes. The apparent extension would vary from night to night depending on the post sunset vertical velocity of the F layer. Over equatorial region background electron density may be playing a vital role in providing the equinoctial asymmetry in the occurrence of ESF irregularities [16].

The effect of equatorial height variation of F region on ionospheric irregularities in the low latitude F region is also an important aspect. The apex height is also contributing in the occurrence of EPBs. Haaser et al. [50] suggested that EPBs occurred near the geomagnetic dip equator (<20° dip), typically within the nighttime ionospheric anomaly, while plasma blobs occurred mainly away from the geomagnetic dip equator, outside the anomaly regions (>15° dip). Yokoyama et al. [51] reported that the zonal structure of the plasma blobs in the northern hemisphere corresponded to that of the topside EPB in the southern hemisphere on a common magnetic flux tube, although the plasma blobs and the EPBs are separated by more than 20° in latitude.

Based on satellite data, Le et al. [52] reported that the localized eastward polarized electric field plays an important role in the creation of EPBs and plasma blobs. The strength of localized eastward polarized electric field is may depend on the virtual height of the F region at dip equator. They are directly proportional to each other. The fluctuations in the virtual height of the equatorial F region creates oscillations of F region in wave nature along the latitudes which is started from the magnetic equator to low latitude (±20°) crest of a wave. The background plasma density and fluctuations in plasma density are important factors for characterizing plasma blobs [53].

The eastward polarized electric field helps to combine flowing plasma with the background plasma over low latitude. Due to this combination, EPBs are generated over low latitude regions. According to literature serve, it is clear that ionospheric irregularities like EPBs or plasma blobs are not observed regularly. This may happen because of low combination or no combination of the plasma. Thus, this combination depends on the strength of eastward polarized electric field. If the strength of eastward polarized electric field is very low, then combinations will not possible while, for its particular value, low energy regions created which are captured in optical data as dark regions. These dark regions are also called as EPBs. If the strength of eastward polarized electric field is very high then, the rate of recombination will increase and high energy regions may create over low latitude regions. These high energy regions cause the enhancement in intensity of OI 630.0 nm emission, called as plasma blobs. The strength of eastward polarized electric field is also depends on the virtual height of F region at dip equator. Our results and analysis

gives strong support for this statement. Herein, one more thing is that the flowing of plasma is in wavy nature, travel from the dip equator to low latitude. This nature of the flowing of plasma also makes an effect on the combination or recombination of plasma over low latitude regions. Thus to explain this nonlinear problem we need of more theoretical models.

4. Conclusions

Understanding of fundamental of EPBs, generation magnesium is very important for better communication and navigation system. Thus, we need more observations to study such phenomenon. In this chapter we have summarized the recent review on observation of EPBs using GPS and ASI.

Acknowledgements

The authors, DPN and SSP are highly indebted to Department of Science and Technology, Science and Engineering Research Board (DST-SERB), Government of India, for providing full financial assistance to carry out the present work under the major research project (File No. EEQ/2016/000275).

Author details

Dada P. Nade*, Swapnil S. Potdar and Rani P. Pawar
Department of Physics, Sanjay Ghodawat University, Kolhapur, India

*Address all correspondence to: dada.nade@gmail.com

References

[1] Abdu MA, Sobral JHA, Nelson OR, Batista IS. Solar cycle related range type spread-F occurrence characteristics over equatorial and low latitude stations in Brazil. Journal of Atmospheric and Terrestrial Physics. 1985;**47**(8-10):901-905

[2] Chapagain NP, Fejer BG, Chau JL. Climatology of postsunset equatorial spread F over Jicamarca. Journal of Geophysical Research: Space Physics. 2009;**114**(7)

[3] Nade DP, Shetti DJ, Sharma AK, Taori A, Chavan GA, Patil PT, et al. Geographical analysis of equatorial plasma bubbles by GPS and nightglow measurements. Advances in Space Research. 2015;**56**(9):1901-1910

[4] Sahai Y, Fagundes PR, Abalde JR, Pimenta AA, Bittencourt JA, Otsuka Y, et al. Generation of large-scale equatorial F-region plasma depletions during low range spread-F season. Annales de Geophysique. 2004;**22**(1):15-23

[5] Nade DP, Nikte SS, Ghodpage RN, Patil PT, Rokade MV, Vhatkar RS. Analysis of plasma bubbles observed in night airglow emission line OI 630.0 nm from Kolhapur using all sky imager. International Journal of Engineering Science Research. 2012;**03**(02):746-750

[6] Weber EJ, Buchau J, Moore JG. Airborne studies of equatorial F layer ionospheric irregularities. Journal of Geophysical Research: Space Physics. 2008;**85**(A9):4631-4641

[7] Sahai Y, Fagundes PR, Bittencourt JA, Abdu MA. Occurrence of large scale equatorial F-region plasma depletions during geo-magnetic disturbances. Journal of Atmospheric and Solar-Terrestrial Physics. 1998;**60**(16):1593-1604

[8] Nade DP, Sharma AK, Nikte SS, Patil PT, Ghodpage RN, Rokade MV, et al. Zonal velocity of the equatorial plasma bubbles over Kolhapur, India. Annales de Geophysique. 2013;**31**(11):2077-2084

[9] Pimenta AA, Fagundes PR, Bittencourt JA, Sahai Y, Gobbi D, Medeiros AF, et al. Ionospheric plasma bubble zonal drift: A methodology using OI 630 mn all-sky imaging systems. Advances in Space Research. 2001;**27**(6-7):1219-1224

[10] Nade DP, Sharma AK, Nikte SS, Chavan GA, Ghodpage RN, Patil PT, et al. Observations of plasma blobs by OI 630 nm using ASI and photometer over Kolhapur, India. Earth, Moon, and Planets. 2014;**112**(1-4):89-101

[11] Sahai Y, Fagundes PR, Bittencourt JA. Transequatorial F-region ionospheric plasma bubbles: Solar cycle effects. Journal of Atmospheric and Solar-Terrestrial Physics. 2002;**62**(15):1377-1383

[12] Sharma AK, Nade DP, Nikte SS, Patil PT, Ghodpage RN, Vhatkar RS, et al. Occurrence of equatorial plasma bubbles over Kolhapur. Advances in Space Research. 2014;**54**(3):435-442

[13] Fejer BG, Scherliess L, de Paula ER. Effects of the vertical plasma drift velocity on the generation and evolution of equatorial spread F. Journal of Geophysical Research: Space Physics. 2003;**104**(A9):19859-19869

[14] Kelley MC, Makela JJ, De La Beaujardiére O, Retterer J. Convective ionospheric storms: A review. Reviews of Geophysics. 2011;**49**

[15] Kakad B, Jeeva K, Nair KU, Bhattacharyya A. Magnetic activity linked generation of nighttime equatorial spread F irregularities. Journal of Geophysical Research: Space Physics. 2007;**112**(7)

[16] Sripathi S, Kakad B, Bhattacharyya A. Study of equinoctial asymmetry in the equatorial spread F (ESF) irregularities over Indian region using multi-instrument observations in the descending phase of solar cycle 23. Journal of Geophysical Research: Space Physics. 2011;**116**(11)

[17] Abalde JR, Fagundes PR, Sahai Y, Pillat VG, Pimenta AA, Bittencourt JA. Height-resolved ionospheric drifts at low latitudes from simultaneous OI 777.4 nm and OI 630.0 nm imaging observations. Journal of Geophysical Research: Space Physics. 2004;**109**(A11)

[18] Shvarts D, Alon U, Ofer D, McCrory RL, Verdon CP. Nonlinear evolution of multimode Rayleigh-Taylor instability in two and three dimensions. Physics of Plasmas. 1995;**2**(6):2465-2472

[19] Huang C, Lu Q, Wu M, Lu S, Wang S. Out-of-plane electron currents in magnetic islands formed during collisionless magnetic reconnection. Journal of Geophysical Research: Space Physics. 2013;**118**(3):991-996

[20] Sidorova LN, Filippov SV. Plasma bubbles in the topside ionosphere: Estimations of the survival possibility. Journal of Atmospheric and Solar-Terrestrial Physics. 2014;**119**:35-41

[21] Pimenta AA, Sahai Y, Bittencourt JA, Rich FJ. Ionospheric plasma blobs observed by OI 630 nm all-sky imaging in the Brazilian tropical sector during the major geomagnetic storm of April 6-7, 2000. Geophysical Research Letters. 2007;**34**(2)

[22] Krall J, Huba JD, Ossakow SL, Joyce G. Equatorial spread F fossil plumes. Annales de Geophysique. 2010;**28**(11):2059-2069

[23] Chen Y, Liu L, Le H. Solar activity variations of nighttime ionospheric peak electron density. Journal of Geophysical Research: Space Physics. 2008;**113**(11)

[24] Choi HS, Kil H, Kwak YS, Park YD, Cho KS. Comparison of the bubble and blob distributions during the solar minimum. Journal of Geophysical Research: Space Physics. 2012;**117**(4)

[25] Kil H, Choi HS, Heelis RA, Paxton LJ, Coley WR, Miller ES. Onset conditions of bubbles and blobs: A case study on 2 March 2009. Geophysical Research Letters. 2011;**38**(6)

[26] Bates DR. Emission of forbidden red and green lines of atomic oxygen from the nocturnal F region. Planetary and Space Science. 1992;**40**(7):893-899

[27] Vlasov MN, Nicolls MJ, Kelley MC, Smith SM, Aponte N, Gonzalez SA. Modeling of airglow and ionospheric parameters at Arecibo during quiet and disturbed periods in October 2002. Journal of Geophysical Research: Space Physics. 2005;**110**(A7)

[28] Otsuka Y, Shiokawa K, Ogawa T, Yokoyama T, Yamamoto M, Fukao S. Spatial relationship of equatorial plasma bubbles and field-aligned irregularities observed with an all-sky airglow imager and the equatorial atmosphere radar. Geophysical Research Letters. 2004;**31**(20)

[29] Garcia FJ, Taylor MJ, Kelley MC. Two-dimensional spectral analysis of mesospheric airglow image data. Applied Optics. 2008;**36**(29):7374

[30] Sekar R, Chakrabarty D, Sarkhel S, Patra AK, Devasia CV, Kelley MC. Identification of active fossil bubbles based on coordinated VHF radar and airglow measurements. Annales de Geophysique. 2007;**25**(10):2099-2102

[31] Kubota M, Fukunishi H, Okano S. Characteristics of medium- and large-scale TIDs over Japan derived from OI 630-nm nightglow observation. Earth, Planets and Space. 2001;**53**(7):741-751

[32] Lakshmi Narayanan V, Gurubaran S, Emperumal K. Imaging observations of upper mesospheric nightglow emissions from Tirunelveli (8.7°N). Indian Journal of Radio & Space Physics. 2009;**38**(3):150-158

[33] Sharma AK, Nade DP, Nikte SS, Ghodpage RN, Patil PT, Rokade MV, et al. Development of fast image analysis technique for all-sky images. Current Science. 2014;**106**(8):1085-1093

[34] Taori A, Jayaraman A, Kamalakar V. Imaging of mesosphere-thermosphere airglow emissions over Gadanki (13.5°N, 79.2°E) - first results. Journal of Atmospheric and Solar-Terrestrial Physics. 2013;**93**:21-28

[35] Dashora N, Pandey R. Observations in equatorial anomaly region of total electron content enhancements and depletions. Annales de Geophysique. 2005;**23**(7):2449-2456

[36] Dow JM, Neilan RE, Rizos C. The international GNSS service in a changing landscape of global navigation satellite systems. Journal of Geodesy. 2009;**83**(3-4):191-198

[37] Browne IC, Evans JV, Hargreaves JK, Murray WAS. Radio echoes from the moon. Proceedings of the Physical Society Section B. 1956;**69**(9):901-920

[38] Nishioka M, Saito A, Tsugawa T. Occurrence characteristics of plasma bubble derived from global ground-based GPS receiver networks. Journal of Geophysical Research: Space Physics. 2008;**113**(5)

[39] Haase JS, Dautermann T, Taylor MJ, Chapagain N, Calais E, Pautet D. Propagation of plasma bubbles observed in Brazil from GPS and airglow data. Advances in Space Research. 2011;**47**(10):1758-1776

[40] Takahashi H, Wrasse CM, Otsuka Y, Ivo A, Gomes V, Paulino I, et al. Plasma bubble monitoring by TEC map and 630nm airglow image. Journal of Atmospheric and Solar-Terrestrial Physics. 2015;**130-131**:151-158

[41] Kumar S, Chen W, Liu Z, Ji S. Effects of solar and geomagnetic activity on the occurrence of equatorial plasma bubbles over Hong Kong. Journal of Geophysical Research: Space Physics. 2016;**121**(9):9164-9178

[42] Okoh D, Rabiu B, Shiokawa K, Otsuka Y, Segun B, Falayi E, et al. First study on the occurrence frequency of equatorial plasma bubbles over West Africa using an all-sky airglow imager and GNSS receivers. Journal of Geophysical Research: Space Physics. 2017;**122**(12):12430-12444

[43] Kumar S. Morphology of equatorial plasma bubbles during low and high solar activity years over Indian sector. Astrophysics and Space Science. 2017;**362**(5)

[44] Takahashi H, Wrasse CM, Figueiredo CAOB, Barros D, Abdu MA, Otsuka Y, et al. Equatorial plasma bubble seeding by MSTIDs in the ionosphere. Progress in Earth and Planetary Science. 2018;**5**(1)

[45] Barros D, Takahashi H, Wrasse CM, Figueiredo CAOB. Characteristics of equatorial plasma bubbles observed by TEC map based on ground-based GNSS receivers over South America. Annales de Geophysique. 2018;**36**(1):91-100

[46] Bumrungkit A, Supnithi P, Saito S. Statistical analysis of separation distance between equatorial plasma bubbles near Suvarnabhumi International Airport, Thailand. Journal of Geophysical Research: Space Physics. 2018;**123**(9):7858-7870

[47] Panda D, Senapati B, Tyagi B, Kundu B. Effects of Rayleigh-Taylor instability and ionospheric plasma bubbles on the global navigation satellite

system signal. Journal of Asian Earth Sciences. 2019;**170**:225-233

[48] Moraes A d O, Vani BC, Costa E, Abdu MA, de Paula ER, Sousasantos J, et al. GPS availability and positioning issues when the signal paths are aligned with ionospheric plasma bubbles. GPS Solutions. 2018;**22**(4)

[49] Rajesh PK, Liu JY, Sinha HSS, Banerjee SB. Appearance and extension of airglow depletions. Journal of Geophysical Research: Space Physics. 2010;**115**(8)

[50] Haaser RA, Earle GD, Heelis RA, Klenzing J, Stoneback R, Coley WR, et al. Characteristics of low-latitude ionospheric depletions and enhancements during solar minimum. Journal of Geophysical Research: Space Physics. 2012;**117**(10)

[51] Yokoyama T, Su SY, Fukao S. Plasma blobs and irregularities concurrently observed by ROCSAT-1 and equatorial atmosphere radar. Journal of Geophysical Research: Space Physics. 2007;**112**(5)

[52] Le G, Huang CS, Pfaff RF, Su SY, Yeh HC, Heelis RA, et al. Plasma density enhancements associated with equatorial spread F: ROCSAT-1 and DMSP observations. Journal of Geophysical Research: Space Physics. 2003;**108**(A8)

[53] Kil H, Kwak YS, Lee WK, Krall J, Huba JD, Oh SJ. Nonmigrating tidal signature in the distributions of equatorial plasma bubbles and prereversal enhancement. Journal of Geophysical Research: Space Physics. 2015;**120**(4):3254-3262